# Notes

Contribution from the Department of Chemistry, Virginia Polytechnic Institute and State University, Blacksburg, Virginia 24061

## Observations on the Formation of $HFe_3(CO)_{11}^-$ on Hydroxylated $\gamma$-$Al_2O_3$

Brian E. Hanson,* Joseph J. Bergmeister III, John T. Petty, and Melissa C. Connaway

*Received November 18, 1985*

The decomposition of iron carbonyls on various refractory supports has demonstrated that very highly dispersed iron particles may be obtained under mild conditions.[1-4] Temperature-programmed decomposition studies[4] suggest that iron subcarbonyls are stabilized on partially dehydroxylated $\gamma$-$Al_2O_3$ when $Fe(CO)_5$, $Fe_2(CO)_9$, or $Fe_3(CO)_{12}$ is adsorbed onto the support. On hydroxylated $\eta$-$Al_2O_3$ or MgO, $HFe_3(CO)_{11}^-$ is readily formed upon adsorption of $Fe_3(CO)_{12}$.[5-7] This anion is reported to be stable to vacuum when supported on aluminum oxide. It has been postulated by others, however, that subcarbonyls of $HFe_3(CO)_{11}^-$ may be formed on aluminum oxide.[8] It is generally accepted that the formation of $HFe_3(CO)_{11}^-$ in basic solution involves nucleophilic attack of hydroxide on coordinated carbon monoxide of $Fe_3(CO)_{12}$.[7,9] On metal oxides, the nucleophile has been postulated to be a surface hydroxyl group.[7]

Hydrocarbon solutions of $Fe_3(CO)_{12}$ are readily decolorized by hydroxylated aluminas to give a brick red solid.[6-8,10,11] Results from proton NMR, infrared spectroscopy, and UV–visible spectroscopy are consistent with formulation of the adsorbed iron carbonyl as $HFe_3(CO)_{11}^-$.[7,10] Very little evolved $CO_2$ is observed during the adsorption; however, this may be due to formation of carbonate on the alumina.[7,12]

The infrared spectrum as obtained by Hugues et al. for $HFe_3(CO)_{11}^-$(ads) on $\eta$-alumina shows a band at 1590 $cm^{-1}$ assigned to a bridging carbonyl.[7] Also observed was $Fe(CO)_5$ in the gas phase during adsorption of $Fe_3(CO)_{12}$.[13] However, they report no evolution of carbon monoxide. Iwasawa et al.[8] report CO evolution during the adsorption of $Fe_3(CO)_{12}$ on $\gamma$-alumina from pentane and fail to see any bridging carbonyl bands in the infrared spectrum. Thus they assign the structure I to the adsorbed carbonyl.[8] Hugues et al. have assigned structure II to the adsorbed anion.[7]

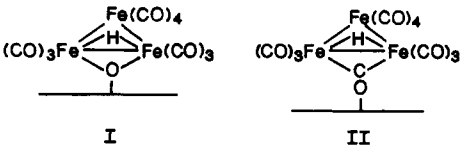


I II

Our results suggest that disproportionation reactions to $HFe_3(CO)_{11}^-$(ads) on hydroxylated $\gamma$-alumina giving $Fe^{2+}$ salts of $[Fe_3(CO)_{11}]^{2-}$ are viable alternatives to nucleophilic attack by surface hydroxyl ion.[13] Once formed on hydroxylated $\gamma$-alumina, the adsorbed anion appears to be susceptible to decarbonylation to yield subcarbonyls that may be represented as $HFe_3(CO)_{11-x}^-$(ads).

### Experimental Section

**General Procedures.** All samples were handled in the absence of air. Gases used were He (99.995), $H_2$ (99.995), and CO (99.99); these were passed over manganous oxide on silica gel to remove traces of oxygen. Pentane was distilled from sodium potassium benzophenone immediately prior to use. Methylene chloride was degassed by three cycles of freeze pump thaw prior to use. Triiron dodecacarbonyl (Pressure Chemical Co.) was recrystallized from pentane and stored under nitrogen in a Vacuum Atmospheres drybox.

The alumina used was CATAPAL SB from Conoco. This was sieved 20–100, 100–200, and >200 mesh in three lots. The alumina was calcined at 450 °C in $O_2$ and then stored in dry air. The alumina was treated further as described below. Gas evolution data is reported for mesh 20–100; IR data is reported for >200 mesh alumina. The surface area is 200 $m^2$ $g^{-1}$.

Hydroxylated alumina surfaces were prepared by passing helium saturated with water over freshly calcined alumina at 100 °C for $^1/_2$ h. The sample was then purged with dry helium for 1 h at 100 °C (flow rate 50 mL/min).

Triiron dodecacarbonyl was dissolved in freshly distilled, degassed pentane and added to the alumina by syringe. Adsorption was conducted either under a flowing helium atmosphere or under a static helium atmosphere with magnetic stirring.

**Helium-Flow Reactor and Estimate of Oxygen Impurity.** The helium-flow system is constructed of $^1/_4$-in. copper tubing, Whitey three-way ball valves, and Nupro bellows valves. The design of the helium-flow system is a modification of that reported by Burwell et al.[14] Compression Swagelok fittings are used to make all connections. Teflon ferrules are used to make connections to glass portions of the system. The fused silica reactors are equipped with Kontes high-vacuum teflon stopcocks to permit transfer of the supported carbonyls to an inert-atmosphere glovebox for IR sample preparation. Two MnO–$SiO_2$ traps are used to remove oxygen from the helium stream. The second of these is placed immediately before the gas enters the reactor.

The oxygen level reaching the reactor was estimated in several blank experiments in which the reactor was charged with a sample of a low weight percent loading MnO–$SiO_2$. By monitoring the oxidation front (MnO to $MnO_2$), we could calculate the total oxygen reaching the reactor. During a 7-h period at a flow rate of 50 mL/min, it was estimated that less than $10^{-7}$ mol of oxygen reached the reactor. Typical iron loadings varied from 5 to 20 mg total $Fe_3(CO)_{12}$ ($1 \times 10^{-5}$–$4 \times 10^{-5}$ mol). Thus for reaction times of 0–10 h, oxidation by trace $O_2$ may be neglected.

**Gas Evolution.** The gases evolved in the reactor were separated by a series of cold traps. The first trap was a condenser, cooled to −196 °C, which collected $CO_2$ and pentane. The second trap was a U-tube packed with Davison-62 silica gel, also cooled to −196 °C, which trapped all other condensable gases, including CO. The third trap consisted of a double U-tube packed with 5A molecular sieves and cooled to −196 °C. Any hydrogen gas was stopped in this trap.

(1) Phillips, J.; Dumesic, J. A. *Appl. Catal.* **1984**, *9*, 1 and references therein.
(2) Nagy, J. B.; Van Eenoo, M.; Derouane, E. G. *J. Catal.* **1979**, *58*, 230.
(3) Hugues, F.; Bussiere, P.; Basset, J. M.; Commereuc, D.; Chauvin, Y.; Bonneviot, L.; Olivier, D. *Proc. Int. Cong. Catal., 7th* Seiyama, T., Tanabe, K., Eds.; Elsevier: Amsterdam, 1981; p 418.
(4) (a) Brenner, A.; Hucul, D. A. *Inorg. Chem.* **1979**, *18*, 2836. (b) Brenner, A.; Hucul, D. A. *J. Am. Chem. Soc.* **1980**, *102*, 2484.
(5) Hugues, F.; Smith, A. K.; Ben Taarit, Y.; Basset, J. M.; Commereuc, D.; Chauvin, Y. *J. Chem. Soc., Chem. Commun.* **1980**, 68.
(6) Commereuc, D.; Chauvin, Y.; Hugues, F.; Basset, J. M.; Olivier, D.; *J. Chem. Soc., Chem. Commun.* **1980**, 154.
(7) Hugues, F.; Basset, J. M.; Ben Taarit, Y.; Choplin, A.; Primet, M.; Rojas, D.; Smith, A. K. *J. Am. Chem. Soc.* **1982**, *104*, 7020.
(8) Iwasawa, Y.; Yamada, M.; Ogasawara, S.; Kuroda, H. *Chem. Lett.* **1983**, 621.
(9) Whitmire, K. H.; Shriver, D. F. In *Comprehensive Organometallic Chemistry*; Abel, E., Stone, F. G. A., Wilkinson, G., Eds.; Pergamon: London, 1983.
(10) Hugues, F. Ph.D. Thesis, Institut de Recherches sur la Catalyse, Villeurbanne, France, 1981.
(11) Alper, H.; Gopal, M. *J. Chem. Soc., Chem. Commun.* **1980**, 821.
(12) (a) Little, L. H. *Infrared Spectra of Adsorbed Species*; Academic: New York, NY, 1966. (b) Parkyns, N. D. *J. Chem. Soc. A* **1969**, 410.
(13) (a) Hieber, W.; Sedlmeier, J.; Werner, R. *Chem. Ber.* **1957**, *90*, 278. (b) Hieber, W. *Adv. Organomet. Chem.* **1970**, *8*, 1. (c) Hieber, W.; Brendel, G. *Z. Anorg. Allg. Chem.* **1957**, *289*, 324. (d) Hieber, W.; Brendel, G. *Z. Anorg. Allg. Chem.* **1957**, *289*, 338.
(14) (a) Bowman, R. G.; Burwell, R. L., Jr. *J. Catal.* **1984**, *88*, 388. (b) Bowman, R. G.; Burwell, R. L., Jr. *J. Catal.* **1980**, *63*, 463. (c) Laniecki, M.; Burwell, R. L., Jr. *J. Colloid Interface Sci.* **1980**, *75*, 95.

0020-1669/86/1325-3089$01.50/0 

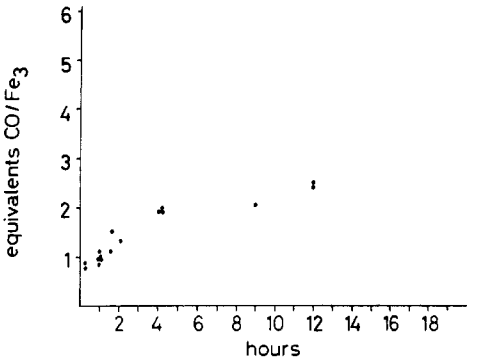


**Figure 1.** Carbon monoxide evolution during the adsorption of $Fe_3(CO)_{12}$ onto hydroxylated $\gamma$-alumina. Each point represents a separate experiment.

The gases were released for analysis by removing the liquid nitrogen Dewar or, in the case of $CO_2$, replacing the liquid nitrogen with a methanol slush (−96 °C). The released gases were separated from any residual atmospheric gases with columns of 80–100 mesh Porapak Q for $CO_2$ and 5A molecular sieves for CO and determined at a GOW MAC thermal conductivity detector. Hydrogen gas was passed through a hot copper oxide column and was determined as water at the TC detector. At reactor temperatures of <50 °C, no hydrogen gas was evolved when $Fe_3(CO)_{12}$ was adsorbed on hydroxylated $\gamma$-alumina.

**Infrared Spectra.** All in situ infrared spectra were recorded on a Nicolet 5DX Fourier transform spectrometer in a cell described previously.[15] Alumina pellets were formed by compressing about 15 mg of powder at 1500 psi in a standard infrared pellet die. The pellet was then mounted in the cell and heated to 100 °C for 1 h under a helium flow to remove any excess water to give a hydroxylated surface.

In a typical experiment, a pentane solution of triiron dodecacarbonyl was added by syringe to the solvent well at the bottom of the apparatus. The iron carbonyl was loaded onto the pellet by immersion of the pellet into the pentane solution. Approximately 30 s were required to obtain sufficient loading to record an infrared spectrum. In some cases, additional immersions were necessary to obtain sufficient signal to noise. The infrared spectrum of the adsorbed carbonyl was monitored as a function of time under either a static helium atmosphere, helium flow, or vacuum.

## Results

**Gas Evolution.** The technique used for determining evolved gases is outlined in the Experimental Section. At temperatures below 50 °C, hydrogen evolution is not observed during these experiments. All of our experiments were performed in the range 22–26 °C. In addition to carbon monoxide evolution and quantitation, a determination of iron pentacarbonyl present in the solvent trap was also made. Analysis by UV spectroscopy was unreliable due to the volatility of the carbonyl; therefore, iron analyses were performed by digestion of the carbonyl in aqua regia followed by atomic absorption spectroscopy.

Figure 1 shows the CO evolution during adsorption of $Fe_3(CO)_{12}$ as a function of the time of the helium flow. After an initial burst of CO, ca. 1 $CO/Fe_3(CO)_{12}$, there is a slow but steady rate of CO loss for several hours. Iron pentacarbonyl formation is significant in all of these experiments. Most of the $Fe(CO)_5$ is removed from the reactor in the first hour. The average for $Fe(CO)_5$ formation over three runs of 4-h duration was 16.5% of the total iron. The ratios of $CO/Fe_3$ shown in Figure 1 represent values based on total $Fe_3(CO)_{12}$ added to the system and are not corrected to account for formation of $Fe(CO)_5$.

When the adsorption is performed under a static atmosphere of helium for 1 h at 25 °C followed by quenching to −10 °C and sweeping out the reactor with helium for 30 min, the following results are observed: total CO evolved, 0.08 $CO/Fe_3$; $Fe(CO)_5$ removed from the reactor, 6% of total iron. Quenching to −10 °C probably keeps much of the $Fe(CO)_5$ in the reactor.

Several experiments were performed in which $HFe_3(CO)_{11}^-$ was introduced directly to the $\gamma$-alumina. These were performed in methylene chloride due to the insolubility of the anion in pentane. The counterion used was $[PPh_3NPPh_3]^+$, $PPN^+$. In a typical run,

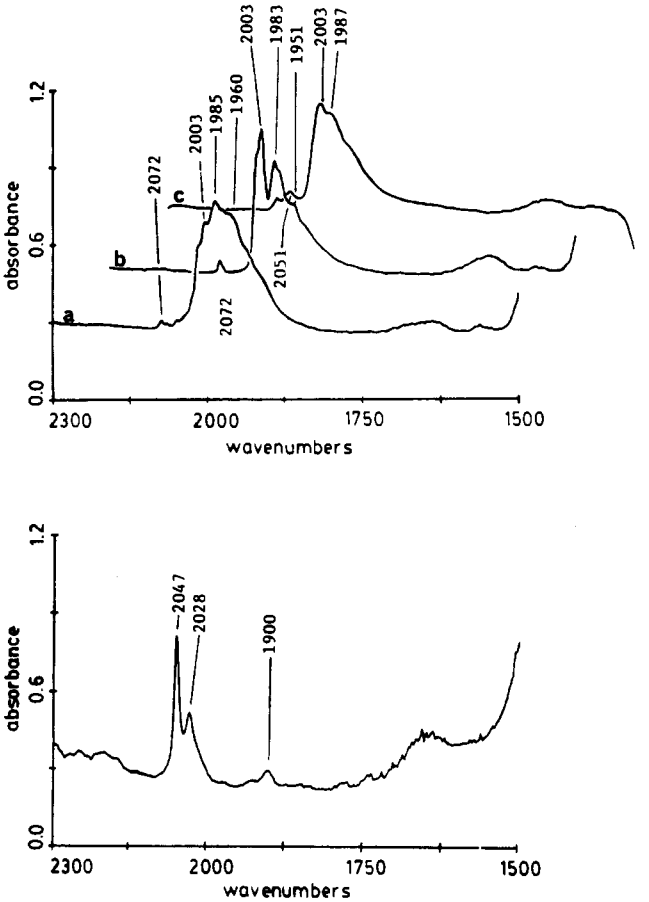


**Figure 2.** In situ infrared spectra for $Fe_3(CO)_{12}$. The top scans show adsorption onto hydroxylated $\gamma$-alumina under static helium atmosphere: trace a, 30 s after immersion; trace b, 15 min after immersion (no further spectral changes observed under helium after 15 min); trace c, same sample after evacuation for 6 min. The lower scan shows adsorption onto $\gamma$-alumina under an atmosphere of carbon monoxide. This trace was recorded 2 min after immersion. No changes are observed as long as the sample remains under CO.

4.18 mg of $[PPN][HFe_3(CO)_{11}]$ in 5 mL of $CH_2Cl_2$ was added to 200 mg of alumina. The average CO evolution for these runs was 0.80 $CO/HFe_3(CO)_{11}^-$ in 1 h of flowing helium. Longer reaction times yielded more evolved CO, indicating a slow steady loss of carbon monoxide. Blank experiments with [PPN]Cl in $CH_2Cl_2$ showed no evolution of carbon monoxide.

**Infrared Spectroscopy.** The infrared spectrum of $HFe_3(CO)_{11}^-$(ads) is very sensitive to sample preparation and handling. Thus we performed FTIR experiments in situ to minimize sample handling and to avoid exposure to air. The infrared spectra were obtained on alumina pellets that had been heated to 100 °C for 1 h in flowing helium to yield a hydroxylated surface. For all spectra shown, the background peaks due to the pellet prior to adsorption of $Fe_3(CO)_{12}$ have been removed by subtraction. The changes in the infrared spectrum following adsorption of $Fe_3(CO)_{12}$ on hydroxylated $\gamma$-alumina under a static helium atmosphere are shown in the top part of Figure 2. Trace 2a is very broad in the terminal carbonyl region and contains bands assignable to $Fe_3(CO)_{12}$ and $Fe(CO)_5$ as well as $HFe_3(CO)_{11}^-$ (vide infra). Trace b represents the spectrum after 15 min and is consistent with $HFe_3(CO)_{11}^-$(ads). No further changes are observed as long as the sample remains under a helium atmosphere.

All the spectra in the top part of Figure 2 show a broad peak centered at approximately 1640 $cm^{-1}$. Although the position of the bridging carbonyl for $HFe_3(CO)_{11}^-$ varies from 1620 to 1760 $cm^{-1}$ in solution as a function of solvent and cation,[16] we do not

(15) Connaway, M. C.; Hanson, B. E. *Inorg. Chem.* **1986**, *25*, 1445.

(16) (a) Cheng, C.-H.; Chen, C. *Inorg. Chem.* **1983**, *22*, 3378. (b) Shick, K.-P.; Jones, N. L.; Sekula, P.; Boag, N. M.; Labinger, J. A.; Kaesz, H. D. *Inorg. Chem.* **1984**, *23*, 2204.

**Table I.** CO Stretching Frequencies ($cm^{-1}$) for Iron Carbonyls

| | | | | | | | | | | | |
|---|---|---|---|---|---|---|---|---|---|---|---|
| $Fe_3(CO)_{12}$[a] | | 2054 vs | | 2012 vs | | | 1955 | | | 1852 | 1821 | |
| $(Et_4N)HFe_3(CO)_{11}$[a] | 2067 w | | | | 2001 s | 1981 s | 1953 s | 1932 s | | | | 1741 s |
| $Fe(CO)_5$[a] | | | 2022 | | 2000 | | 1943 vs | | 1913 m | | | |
| $(PPN)_2Fe_3(CO)_{11}$[a] | | 1943 | | | | | | | | | | |
| $(PPN)(HFe_4(CO)_{13})$[a] | 2072 w | | 2031 | | | 1984 | 1961 | 1936 | | | | |
| in situ | | | | | | | | | | | | |
| $HFe_3(CO)_{11}$(ads) | 2072 w | | | | 2003 s | 1983 s | 1951 w | | | | | |
| $Fe(CO)_5$(phys) | | | 2024 s | | 2003 s | | | | | | | |
| $PPN^+HFe_3(CO)_{11}^-$ | 2072 w | | | | 2004 s | 1979 s | 1951 w | | | | | |
| $Fe_3(CO)_{12}$(phys) | | 2047 | 2028 | | | | | | 1900 | | | |

[a] From ref 9 and citations therein.

assign this band to a bridging carbonyl. It appears to be due either to residual water on the alumina surface that is poorly subtracted or to carbonate. If air is introduced intentionally to a sample containing the 1640-$cm^{-1}$ band, this band remains unchanged or grows slightly in intensity while all the carbonyl bands are lost due to oxidation of the sample. Trace c represents the spectrum after evacuating the infrared cell for 6 min. Much of the resolution is lost in this spectrum, and it is likely that many species exist on the surface after evacuation. A new band at 2048 $cm^{-1}$ appears in this spectrum, which is consistent with the formation of a new carbonyl species. Evacuation of the sample used in Figure 2 did not produce any new bands in the bridging carbonyl region as seen in trace 2c.

The effect of gas-phase CO on the adsorption of $Fe_3(CO)_{12}$ on hydroxylated alumina is shown in the lower part of Figure 2. After immersion of the pellet to load the alumina with $Fe_3(CO)_{12}$ the spectrum consists of two bands in the terminal carbonyl region. These correspond closely to the bands reported for $Fe_3(CO)_{12}$ physisorbed on silica gel.[17] This spectrum remains unchanged as long as the sample remains under CO. *Thus, carbon monoxide inhibits formation of anionic species as well as of $Fe(CO)_5$.* The spectrum of gas-phase CO is not observed since the background spectrum was recorded with the same CO atmosphere.

In Figure 3 (top) a series of spectra are shown for a sample that was sandwiched between two additional salt plates; otherwise, the sample was handled as for Figure 2 (top). The chemistry associated with the adsorption of $Fe_3(CO)_{12}$ on $\gamma$-alumina in this experiment is slower than that shown in Figure 2. This is probably due to local CO partial pressure between the salt plates since, as shown in the lower trace of Figure 2, CO inhibits anion formation. With time, a complex series of changes are observed in this sample. The initial spectrum, 3a (top), shows the presence of $Fe_3(CO)_{12}$(ads), bands at 2048 and 2024 $cm^{-1}$ (compare Figure 2), and a band at 2000 $cm^{-1}$. At this point the sample is green. With time, two bands at 2024 and 2000 $cm^{-1}$ grow in intensity and a broad shoulder is observed below 2000 $cm^{-1}$ as the $Fe_3(CO)_{12}$ band at 2048 $cm^{-1}$ decreases in intensity. After 15 min, the sample begins to take on a red color. The bands of 2024 and 2000 $cm^{-1}$ are clearly due to $Fe(CO)_5$; vide infra. Iron pentacarbonyl has also been observed by IR spectroscopy during the gas-phase adsorption of $Fe_3(CO)_{12}$ on silica gel[17] and on $\eta$-alumina.[13] After 2 h, the $Fe(CO)_5$ peaks have disappeared and the spectrum is virtually identical with that in Figure 2b (top). It should be noted that, in some experiments using this sandwich technique, a bridging carbonyl at 1695 $cm^{-1}$ is observed. This band is seen in Figure 3 (top). However, it is not seen in all samples handled in this manner. If the 1695-$cm^{-1}$ band is a bridging carbonyl, its appearance is very sensitive to reaction conditions. In all samples in which the 1695-$cm^{-1}$ band is observed, it is removed by evacuation of the sample as seen in Figure 3e (top).

When $Fe(CO)_5$ is adsorbed onto $\gamma$-alumina from pentane, the spectra shown in Figure 3 (bottom) are obtained. The two bands at 2024 and 2002 $cm^{-1}$ in the first trace confirm the assignment of $Fe(CO)_5$ to the same bands in Figures 2a and 3a–c (top). After several hours, the spectrum, trace 3b (bottom), is substantially different from that obtained from the adsorption of $Fe_3(CO)_{12}$ on alumina (Figures 2b and 3d (top)). Thus, $Fe(CO)_5$ and $Fe_3(CO)_{12}$ do not appear to give the same products upon adsorption on hydroxylated $\gamma$-alumina. Also, $Fe(CO)_5$ reacts at a much slower rate with $\gamma$-alumina than does $Fe_3(CO)_{12}$. The general decrease in intensity with time in Figure 3 is probably due to some loss of $Fe(CO)_5$ from the pellet before it is able to react with the alumina surface. The spectrum obtained here may be consistent with the tetranuclear anion $HFe_4(CO)_{13}^-$. (See Table I for a complete list of carbonyl bands.)

The anion, $HFe_3(CO)_{11}^-$, may be directly introduced to the alumina surface as the PPN (bis(triphenylphosphine)nitrogen-

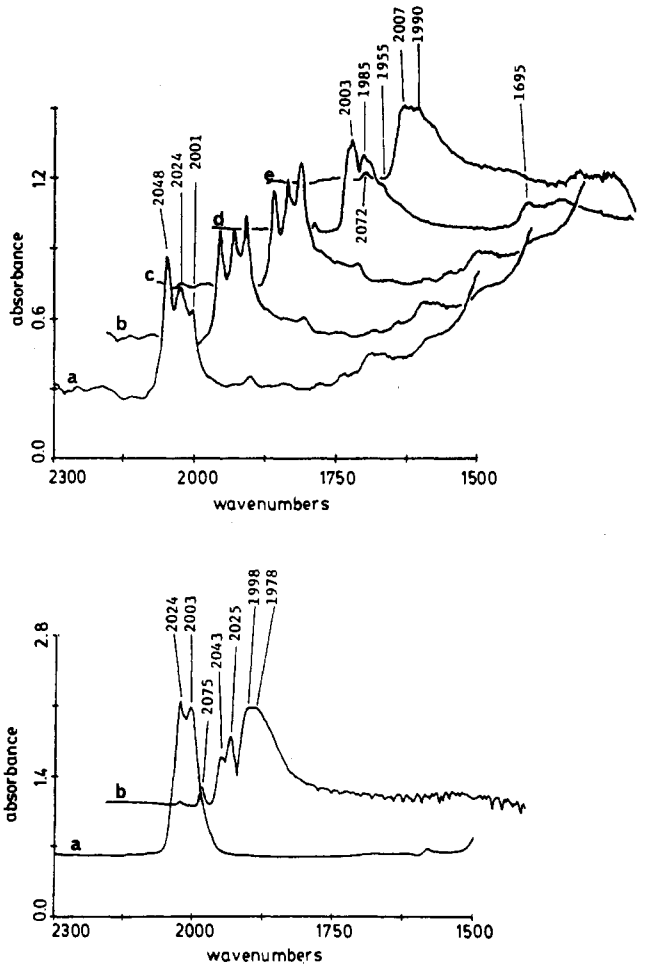


**Figure 3.** In situ infrared spectra. The top scans show adsorption of $Fe_3(CO)_{12}$ onto a wafer of hydroxylated alumina sandwiched between two salt plates: trace a, 5 min after immersion; trace b, 10 min after immersion; trace c, 15 min after immersion. After 2 h a steady-state spectrum is observed. This is shown in trace d. Trace e represents the spectrum after evacuation for 6 min. The lower scans show adsorption of $Fe(CO)_5$ onto hydroxylated $\gamma$-alumina from pentane: trace a, 30 s after immersion; trace b, steady-state spectrum 2 h after immersion. The ordinate scale of trace b is expanded by a factor of 2 relative to trace a.

(17) (a) Trusheim, M. R.; Jackson, R. L. *J. Phys. Chem.* **1983**, *87*, 1910. (b) Jackson, R. L.; Trusheim, M. R. *J. Am. Chem. Soc.* **1982**, *104*, 6590.

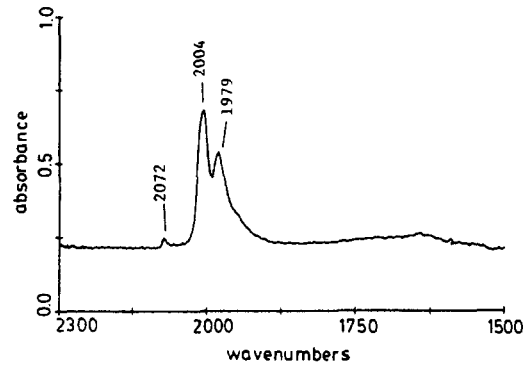


**Figure 4.** Infrared spectrum obtained for $HFe_3(CO)_{11}^-$ adsorbed onto hydroxylated $\gamma$-alumina as the PPN salt from $CH_2Cl_2$.

(1+)) salt. Figure 4 shows the infrared spectrum of $HFe_3(CO)_{11}^-$ on alumina after adsorption from $CH_2Cl_2$. (Methylene chloride is the solvent in this experiment since the salt, $[PPN][HFe_3(CO)_{11}]$, is not soluble in pentane.) This spectrum shows a remarkable similarity to that obtained in Figures 2b (top) and 3d (top). The absence of a bridging carbonyl band may be due to the inherent weakness of this band. Another possibility is that the anion rapidly decarbonylates to form a subcarbonyl that lacks a bridging CO group. The anion $HFe_3(CO)_{11}^-$ does slowly lose carbon monoxide when directly adsorbed onto alumina (vide supra); however, it is unlikely that in the time frame of the experiment in Figure 4, i.e., 2 min, that all adsorbed anions have lost their bridging carbonyl.

Significantly, no $Fe(CO)_5$ is observed in the infrared spectra obtained after adsorption of the anion. Thus, $Fe(CO)_5$ is not a decomposition product of $HFe_3(CO)_{11}^-$ but is formed either concurrently with or prior to $HFe_3(CO)_{11}^-$ in a reaction sequence starting with $Fe_3(CO)_{12}$.

## Discussion

**Possible Routes to $HFe_3(CO)_{11}^-$(ads).** The most striking observations from the discussion in the previous sections are (1) that $Fe(CO)_5$ is always formed concurrently with $HFe_3(CO)_{11}^-$ on hydroxylated alumina and (2) that CO pressures inhibit formation of both $Fe(CO)_5$ and $HFe_3(CO)_{11}^-$.

These facts cannot be explained by simple nucleophilic attack of surface hydroxyl on coordinated CO. It is possible for carbon monoxide to inhibit this reaction only if it binds strongly to the surface of aluminum oxide. Also, it was shown in Figure 4 that $HFe_3(CO)_{11}^-$ is not a precursor to iron pentacarbonyl on alumina at ambient temperature. It should be noted that Brenner and Hucul do not observe $Fe(CO)_5$ during adsorption of $Fe_3(CO)_{12}$ on partially dehydroxylated alumina.[4] Formation of $Fe(CO)_5$ appears to be unique to hydroxylated surfaces.

The disproportionation reactions reported by Hieber[13] give a clue for both CO inhibition and formation of iron pentacarbonyl. Although the reversibility of the disproportionation reactions (eq 1–4, showing potential stoichiometries) has not been demonstrated experimentally, it is reasonable to expect that these reactions proceed in a stepwise fashion in which CO loss is important early in the reaction sequence.[18,19] Also, the large quantities of CO released in reaction 1 may react with $Fe_3(CO)_{12}$ or oxidized iron compounds to yield $Fe(CO)_5$. In the presence of a proton source, formation of the hydrido anion, $HFe_3(CO)_{11}^-$, will be favored. These reactions are balanced by showing water on the left hand side of the equations for consistency; however, they may also be balanced with either hydroxyl or protons on the left as appropriate.

$$4Fe_3(CO)_{12} + 3H_2O + 18L \rightarrow 3HFe_3(CO)_{11}^- + 3FeL_6^{2+} + 3OH^- + 15CO \quad (1)$$

$$4Fe_3(CO)_{12} + 2H_2O + 12L \rightarrow 3HFe_3(CO)_{11}^- + 2FeL_6^{2+} + Fe(CO)_5 + OH^- + 9CO + CO_2 \quad (2)$$

$$4Fe_3(CO)_{12} + H_2O + 6L \rightarrow 3HFe_3(CO)_{11}^- + FeL_6^{2+} + 2Fe(CO)_5 + H^+ + 3CO + 2CO_2 \quad (3)$$

$$2Fe_3(CO)_{12} + H_2O + 6L \rightarrow HFe_3(CO)_{11}^- + FeL_6^{2+} + OH^- + 2Fe(CO)_5 + 3CO \quad (4)$$

An important feature of these reactions is that in each case CO evolution accompanies formation of $HFe_3(CO)_{11}^-$. Thus, the observation of large quantities of evolved CO may be explained without postulating the formation of subcarbonyls of $HFe_3(CO)_{11}^-$(ads). However, it is clear from the adsorption of $HFe_3(CO)_{11}^-$ that subcarbonyls are ultimately generated (vide supra). Three of these reaction pathways also show the formation of iron pentacarbonyl (eq 2–4) and thus can account for the observation of this molecule during adsorption. It is important to note that the methanol disproportionation of $Fe_3(CO)_{12}$ leads to large quantities of $Fe(CO)_5$—up to 55% of the total iron.[13]

All of the disproportionation reactions, eq 1–4, require the formation of $Fe^{II}L_6$. This is most likely to contain high-spin iron(II). Magnetic susceptibility measurements on samples sealed in helium using the Faraday balance technique indicate a slight paramagnetism. However, the samples have a very large diamagnetic contribution from the glass ampules, and therefore these results should be treated with caution. So far, EPR experiments have failed to give definitive evidence for iron cations on the alumina. Pathways to $HFe_3(CO)_{11}^-$ and $HFe_4(CO)_{13}^-$ via disproportionation of $Fe(CO)_5$ also exist.[9] In these, the disproportionating ligand is taken to be either surface oxide, hydroxyl, or residual water to satisfy the coordination of $Fe^{2+}$ formed in the reaction.

A combination of the reactions of $OH^-$ with $Fe_3(CO)_{12}$ and reactions 1–4 can account for all observed products, i.e., $Fe(CO)_5$, CO, $CO_2$, and $HFe_3(CO)_{11}^-$. Iron pentacarbonyl formed during the initial adsorption of $Fe_3(CO)_{12}$ may then react further to yield either $HFe_3(CO)_{11}^-$ or $HFe_4(CO)_{13}^-$ on the surface.

The CO evolution studies in which $HFe_3(CO)_{11}^-$ is adsorbed directly onto the alumina are consistent with formation of subcarbonyls of $HFe_3(CO)_{11}^-$(ads). Although an exact stoichiometry cannot be assigned for a subcarbonyl, structure I (vide supra) for $HFe_3(CO)_{10}^-$(ads) is a likely candidate for the surface species. This structure accounts for the lack of a distinct bridging carbonyl band for many of these samples.

## Summary

A variety of reaction pathways may lead to $HFe_3(CO)_{11}^-$(ads) on hydroxylated surfaces, but only certain disproportionation reactions can account for CO evolution as well as for $Fe(CO)_5$ formation during the adsorption process. Furthermore, $Fe(CO)_5$ formation occurs concomitantly with the generation of ionic species. As much as 18% of the total iron added to the alumina may leave the reactor as $Fe(CO)_5$ under a helium purge. Disproportionation reactions also are consistent with CO inhibition during the adsorption and the formation of paramagnetic species on the surface. The bridging carbonyl of the adsorbed anion is difficult to observe but is seen at 1695 $cm^{-1}$ on some $\gamma$-alumina samples and at 1590 $cm^{-1}$ on $\eta$-alumina.[7] Evidence from CO evolution data show that subcarbonyls, $HFe_3(CO)_{11-x}$, are ultimately formed.

**Acknowledgment.** Support for this work was provided by the NSF (Grant DMR-8211111). The infrared spectrometer was purchased with funds from the Virginia Mining and Minerals Resources Research Institute. We thank Jim Rancourt for assistance with the magnetic susceptibility experiments.

**Registry No.** $Fe_3(CO)_{12}$, 17685-52-8; $HFe_3(CO)_{11}^-$, 55188-22-2; $Fe(CO)_5$, 13463-40-6; CO, 630-08-0.

(18) The disproportionation reaction of $Fe_3(CO)_{12}$ in methanol does show a rate inhibition when the reaction is performed in CO-saturated methanol.[19]

(19) Bergmeister, J. J., Jr.; Hanson, B. E., work in progress.